Available online at www.sciencedirect.com
ScienceDirect
Thin Solid Films 515 (2006) 2009 – 2014
thin solid films
www.elsevier.com/locate/tsf

Wettability of TiAlN films by molten aluminum

Ping Shen [a,b,*], Masateru Nose [c], Hidetoshi Fujii [a], Kiyoshi Nogi [a]

[a] Joining and Welding Research Institute, Osaka University, 11-1 Mihogaoka Ibaraki, Osaka, 567-0047, Japan
[b] Key Laboratory of Automobile Materials, Department of Materials Science and Engineering, Jilin University, No. 5988 Renmin Street, Changchun, 130025, P. R. China
[c] Department of Industrial Art and Craft, Takaoka National College, 180 Futagami-machi, Takaoka City, Toyama 933-8588, Japan

Received 29 June 2005; received in revised form 5 April 2006; accepted 7 April 2006
Available online 22 June 2006

Abstract

In this study, we made an attempt to measure the wettability of the TiAlN films by molten Al at temperatures between 1073 K and 1273 K using an improved sessile drop method. The true contact angles cannot be obtained for the films deposited on the stainless steel and tungsten substrates due to considerable interdiffusion or reaction between molten Al and the substrate constituents. For the films deposited on the stable alumina single crystals and in contact with clean Al, the true contact angles are possible in the range of 80–100° at 1173–1273 K and the work of adhesion is 0.77–1.08 J m^{-2}. In the case of oxidized Al, typically at $T<1173$ K, however, the wettability and the adhesion are significantly decreased.
© 2006 Elsevier B.V. All rights reserved.

Keywords: Wetting; Adhesion; Oxidation; Interfaces

1. Introduction

A considerable effort has been made in recent years to develop new wear resistant coatings for metal casting or extrusion dies and TiAlN films are one of the most promising candidates due to their high hardness and good resistance to wear, oxidation and corrosion. A large number of papers have been published with regard to these properties [1–12], however, to the best of our knowledge, only a few [13,14] were concerned with the reaction and sticking or adhesion between the TiAlN films and working materials, such as aluminum in aluminum die casting, when the dies are operated at elevated temperatures, which, in practice, are critical problems limiting the lifetime and performance of the dies as well as the quality of the products.

This study presents an attempt to assess the reactivity, wettability and adhesion between the TiAlN film and molten Al by measurement of the contact angles using a sessile drop method. The wettability is characterized by the contact angle, θ, according to Young's equation

$$\sigma_{sv} = \sigma_{sl} + \sigma_{lv}\cos\theta \qquad (1)$$

and the adhesion by the work of adhesion, W_{ad}, following the Young–Dupré equation

$$W_{ad} = \sigma_{lv}(1 + \cos\theta) \qquad (2)$$

where σ_{sv}, σ_{sl} and σ_{lv} are the solid–vapor, solid–liquid and liquid–vapor interfacial free energies, respectively. Similar method was also adopted by Moore et al. [13,14], who determined the wettability of up to fourteen film candidates coated on the H13 steel substrates for Al die casting dies by three molten aluminum alloys and identified the best coating for each alloy using a wettability index. Their results, however, are superficial, and to a great extent, doubtful because of the unsuitable substrates (namely, the H13 steel) used, as will be demonstrated and described in this article.

* Corresponding author. Postal address: Key Laboratory of Automobile Materials, Ministry of Education, and Department of Materials Science and Engineering, Jilin University, No. 5988 Renmin Street, Changchun, 130025, P. R. China. Tel./fax: +86 431 5094699.
E-mail address: shenping@jlu.edu.cn (P. Shen).

0040-6090/$ - see front matter © 2006 Elsevier B.V. All rights reserved.
doi:10.1016/j.tsf.2006.04.036

2. Experimental details

2.1. TiAlN film preparation

Three kinds of mirror-polished substrates were used for deposition of the TiAlN films: SUS 304 plates (25 mm × 25 mm × 1.5 mm), tungsten plates (25 mm × 25 mm × 2 mm, 99.9% purity) and R(01$\bar{1}$2)-facet alumina single crystal wafers (ϕ 20 mm × 1 mm, 99.99% purity). Before deposition, these substrates were ultrasonically cleaned by immersion in acetone, ethanol and 2-propanol in sequence. Two rectangular plates (100 mm × 160 mm × 10 mm, 99.8% purity) of sintered $Ti_{50}Al_{50}$ alloy were sputtered in a mixture of highly purified argon and nitrogen gases, both of 99.9999% purity.

Except for specifically indicated, the TiAlN films were prepared by a DC reactive sputtering (RS) technique using a Facing Targets-type Sputtering system (Osaka Vacuum Co., Ltd.). Detailed experimental conditions are given in Table 1. The depositions were always carried out just after the substrate surface cleaning treatments.

The crystalline phases of the deposited films were identified by X-ray diffractometry (XRD) using Cu Kα radiation with either a thin film method (glancing incidence mode) or a $\theta \sim 2\theta$ goniometer (X'pert system, Philips). The compositions of the constituent elements were determined by wave dispersive spectrometry (JXA-8100, JEOL) and the typical value was $Ti_{25.7}Al_{21.3}N_{53.0}$ (in atomic percent). The error of the film compositions in different samples was estimated to be within ±0.5%. The film thickness and surface roughness (Ra) were measured by a surface profilometer (Dektek 3, Veeco Instrument, Inc., NY, USA).

2.2. Sessile drop experiment

An improved sessile drop method in a non-impingement mode, described in detail elsewhere [15], was employed for the measurement of the contact angle. Before the experiment, a pure (99.99%) aluminum sample, in the form of a small wire segment (ϕ=3 mm) weighing between 0.14 and 0.16 g, was first chemically cleaned in a 20 wt.% NaOH distilled-water solution to remove its surface oxide film. The Al sample and the TiAlN film substrate were then separately immersed in acetone and ultrasonically cleaned. Subsequently, the TiAlN film substrate was placed in a stainless-steel chamber and adjusted to a horizontal position, whereas the Al sample was placed in a glass tube located outside the chamber. The glass tube was connected to an alumina dropping tube (99.6 wt.% purity) with a ϕ=1 mm hole at its bottom, through which the Al sample could be transferred into the chamber and then dropped onto the film substrate when the desired testing temperature was reached, as described below. A schematic diagram showing this apparatus was given in Fig. 2 of Ref. [16].

The chamber was heated in a vacuum (~5 × 10^{-4} Pa) at a rate of 20 K/min up to the testing temperatures (1073–1273 K), at which a purified Ar–3% H_2 gas with an oxygen partial pressure of the order of 10^{-18} Pa (measured by an oxygen sensor of ZrO_2–11 mol% CaO solid electrolytes at 1073 K) was introduced. The atmospheric pressure inside the chamber was controlled at ~1.2 × 10^5 Pa. After the temperature and the atmosphere had stabilized, the Al sample was inserted into the bottom of the alumina tube and held for 40 s in order for it to melt. The molten aluminum was then forced out through the small hole by the pressure difference between inside of the chamber and inside of the alumina tube created by the gas outflow. The oxide film covering the Al surface, if not completely removed by the chemical cleaning, was mechanically removed as the molten aluminum passed through the small hole. The TiAlN film substrate was then slightly lowered for the extruded Al to detach from the alumina tube. At the same time, a high-resolution (2000 × 1312 pixels) photograph was taken and defined as the drop profile at zero time. Subsequent photographs were taken at certain intervals.

After the wetting experiments, the captured drop profiles were analyzed by an axisymmetric-drop-shape analysis program to calculate the contact angles. Selected samples were sectioned perpendicular to the interface and carefully polished to prepare the metallographic specimens. Interfacial microstructures were examined using an environmental scanning electron microscope (Nikon Co., Kanagawa, Japan) with X-ray energy dispersive microanalysis capability.

Table 1
Experimental conditions in the RS deposition

Substrate type	W and Al_2O_3
Target purity	99.8%
Target size (mm)	100 × 160 × 10
Bias voltage (V)	0
Time (h)	~3
Current (A)	2.2
Gas purity (%)	Ar, N_2: 99.9999
Gas flowing rate (× 10^{-6} m^3 min^{-1})	Ar: 10; N_2: 25
Film thickness (μm)	2.5–3.0
Base pressure (Pa)	5 × 10^{-5}
Deposition pressure (Pa)	0.2
Substrate temperature (K)	473
Target-to-substrate distance (mm)	115

3. Results

3.1. Film characterization

Fig. 1 shows the XRD pattern of the Ti–Al–N film, which was determined by the thin film method (glancing incidence

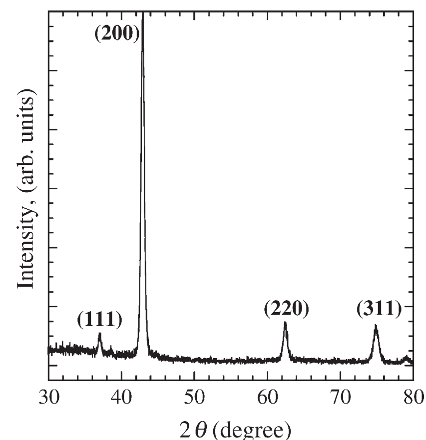

Fig. 1. X-ray diffraction pattern of the TiAlN film in a glancing incidence mode.

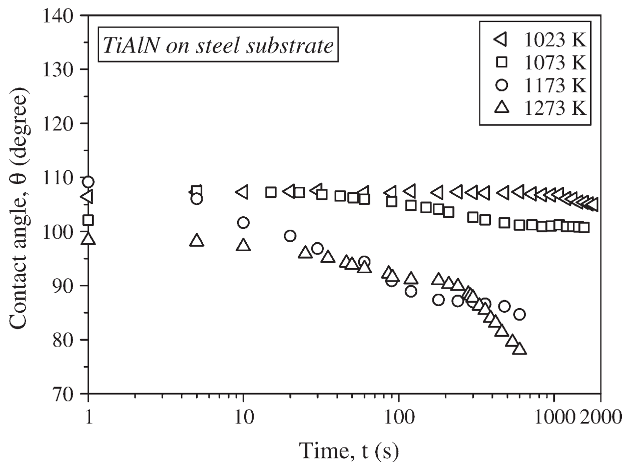

Fig. 2. Variation in the contact angles with time for molten Al on the TiAlN films (Ra = 103 nm) deposited on the flat SUS 304 substrates using the AIP method.

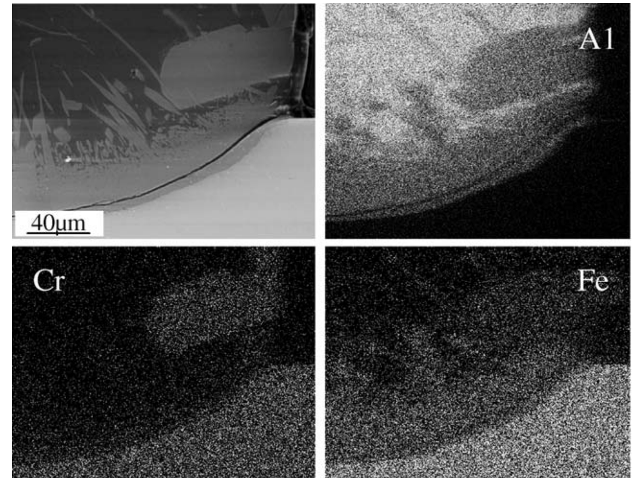

Fig. 4. Microstructure at the Al-film–steel interface and elemental mapping graphs (the sample was tested at 1073 K for 30 min).

mode). The XRD pattern reveals the presence of only one phase that can be assigned to the cubic B1 NaCl-type structure. The grain size of the film, as estimated from the width of the (200) peak using Scherre's equation [17], is about 15 nm.

3.2. Wetting behavior

Fig. 2 shows the variation in the contact angles with time for the molten Al on the TiAlN films deposited on the flat SUS 304 substrates by an arc-ion-plating (AIP) method, which produces the films with relatively large surface roughness (Ra = 103 nm). Non-wetting ($\theta > 90°$) was observed at $T \leq 1073$ K and a transition from the non-wetting to wetting ($\theta < 90°$) appeared at $T > 1073$ K after a short time. The dependence of the contact angle on both the temperature and time implies a strong interaction or a chemical reaction between the molten aluminum and the film or the substrate. In fact, the reaction was perceptible in the real time observations of the change in the drop configuration at the triple junctions, as indicated in Fig. 3, and was further validated by the interfacial microstructural examination (see Fig. 4) after the experiments.

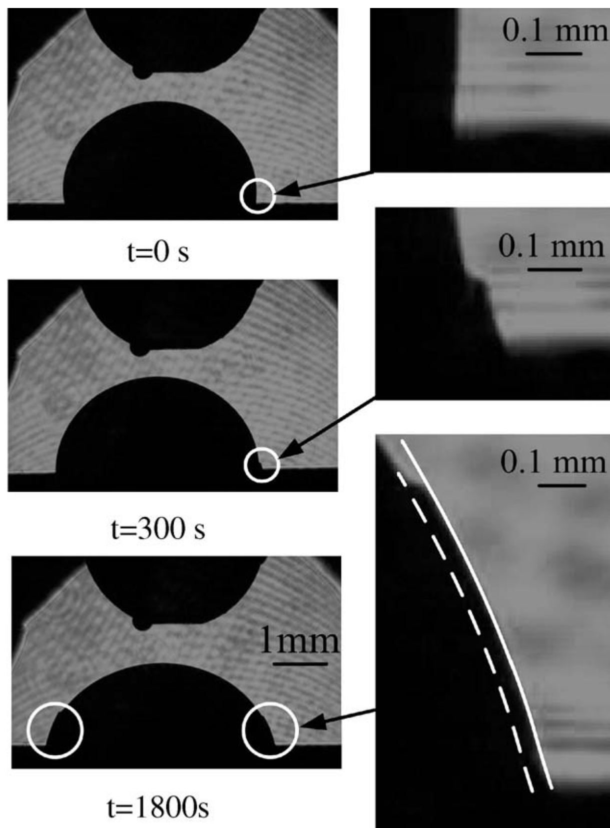

Fig. 3. Representative photographs showing the change in the drop configuration at the triple junctions.

Because of the extensive reaction between molten Al and the steel substrates, the TiAlN film was then deposited on tungsten substrates using the RS method, which provides the higher quality of the films (e.g., the surface roughness of the films produced by RS is much smaller than that by AIP). The reason why we selected tungsten is based on the consideration that

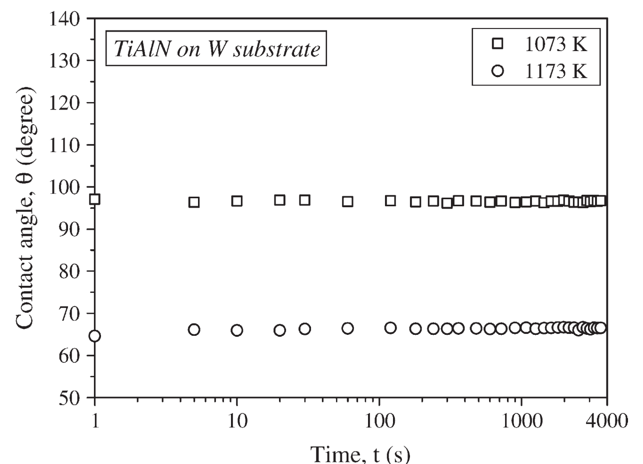

Fig. 5. Variation in the contact angles with time for molten Al on the TiAlN films (Ra = 59 nm) deposited on the W substrates (Ra = 44 nm) using the RS method.

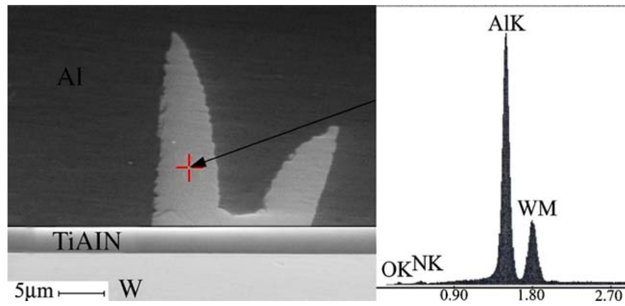

Fig. 6. Microstructure at the Al-film–W interface tested at 1173 K after 60 min. Energy dispersive spectrometry (EDS) shows that the reaction product is Al–W intermetallic compound.

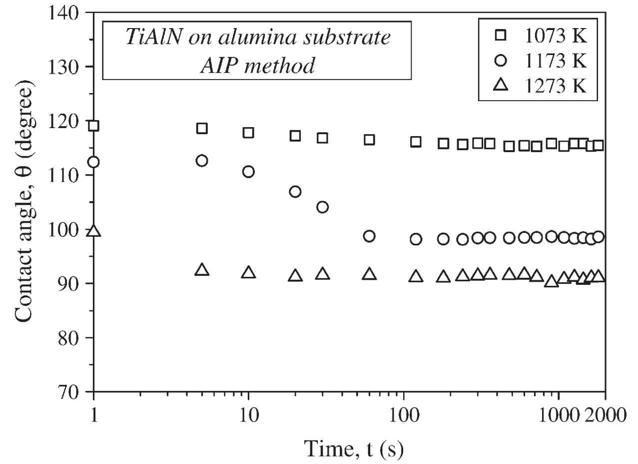

Fig. 8. Variation in the contact angles with time for molten Al on the rough surfaces (Ra=95 nm) of the TiAlN films deposited on the flat alumina single crystals (Ra=3 nm) using the AIP method.

tungsten is a hard and stable metal and possesses good adhesion with the TiAlN film. The wetting results, as shown in Fig. 5, however, are somewhat disappointing. Although the contact angles remain constant during the entire isothermal dwells, the values at 1073 K and 1173 K differ significantly. Microstructure examinations revealed that at 1173 K, some Al–W intermetallic compounds were formed at the interface (see Fig. 6). At 1073 K, although no visible Al–W intermetallics were detected, the interdiffusion between Al and W through the TiAlN film did proceed, as shown in Fig. 7. In this context, W is also not a suitable substrate for depositing the TiAlN film in order to accurately measure the wettability of TiAlN by the molten Al.

Considerable efforts were then made to prepare the TiAlN films deposited on the very flat (Ra=3 nm) alumina single crystal wafers and two kinds of the films were produced: (i) with a thin (0.2–0.3 μm) TiN intermediate layer in order to enhance the adhesion between the TiAlN film and the Al_2O_3 substrate produced by the AIP method, and (ii) without any intermediate layer, namely, directly depositing the film on the alumina substrates by the RS method. The contact angle results are shown in Figs. 8 and 9, respectively, for these two kinds of the films. Repeated experiments were performed only on film (ii) since it has much smaller surface roughness (Ra=10 nm) compared with film (i) (Ra=95 nm). As indicated, a non-wetting behavior generally appears at 1073 K and the contact angles do not show a significant decrease with time. An increase in temperature, however, leads to a considerable decrease in the contact angle as well as a time-dependent decreasing behavior in the initial wetting stages (typically at $t<100$ s), especially for Al on film (ii), where a non-wetting to wetting transition appears. On film (i), although the contact angles display a similar decreasing behavior, they are higher than 90° due to much larger surface roughness.

Fig. 10 shows the microstructures for the samples tested at 1073 K and 1273 K after 30 min. The films do not seem to be seriously attacked by the molten Al but develop good adhesion with both the alumina substrate and molten Al. No significant reaction products were found at the interfaces in a micron-sized area; however, the diffusion of the film constituents such as Ti

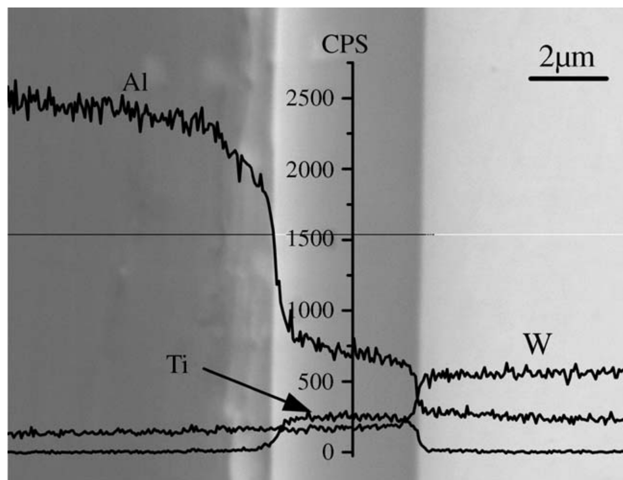

Fig. 7. Microstructure at the Al-film–W interface tested at 1073 K after 60 min. Line scan spectrums show the alterations and relative intensities of Al, Ti and W.

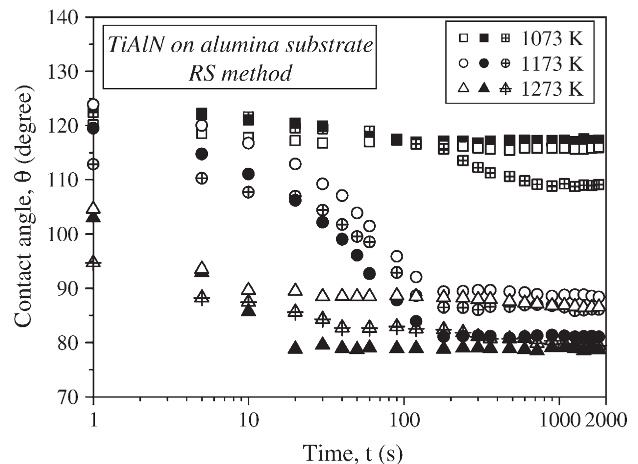

Fig. 9. Variation in the contact angles with time for molten Al on the fine surfaces (Ra=10 nm) of the TiAlN films deposited on the alumina single crystals (Ra=3 nm) using the RS method.

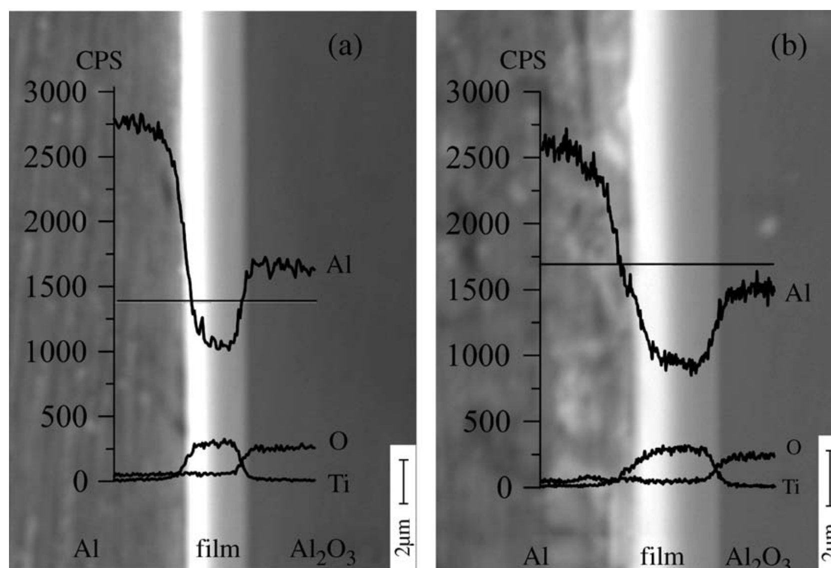

Fig. 10. Microstructures at the Al-film–alumina interface tested at (a) 1073 K and (b) 1273 K after 30 min. Line scan spectrums show the alterations and relative intensities of Al, Ti and O.

into the molten Al seems to progress with the temperature increase.

4. Discussion

The preceding wetting results clearly indicate that the true wettability of the TiAlN films by molten Al cannot be measured for the films deposited on the steel and tungsten substrates. At the temperatures of 1073–1273 K, the interdiffusion and/or the reaction between the substrate constituents and molten Al cannot be inhibited by the TiAlN film, which substantially affect the wetting results. The interdiffusion and the reaction could be understood on the basis of the Al–Fe and Al–W phase diagrams [18], where Al has a high solubility in both Fe and W, meaning that the Al atoms, even those in the TiAlN films, can readily diffuse into the steel and W substrates. In contrast, Fe and W have a very limited solubility in solid Al, and thus a small amount of Fe and W diffusion into liquid Al will result in the formation of Al–Fe and Al–W intermetallics after solidification.

The wetting, on the other hand, is strongly dependent on the molten aluminum surface conditions in addition to the TiAlN film surface roughness. Al is very easily oxidized (from the viewpoint of thermodynamics, the oxidation can occur at oxygen partial pressures $p_{O_2} > 10^{-39}$ Pa at 1073 K and $> 10^{-34}$ Pa at 1173 K [19]) and a very thin oxide film can practically impede the establishment of a true metal–substrate interface. As a result, large apparent contact angles are usually observed, as manifested in many of the studies on the classical Al–Al_2O_3 system [16,20–23]. In this study, although the initial oxide film covering the Al surface was disrupted by the mechanical extrusion of the liquid through the small hole, the formation of the new oxide film during the course of the dropping (it took about 10 s for the extruded Al to detach from the alumina tube) and/or the isothermal dwells could not be prevented since the real p_{O_2} in the furnace is beyond the thermodynamic values for the Al surface deoxidation, particularly at relatively low temperatures. Our previous study [16] has demonstrated that under the present experimental conditions, the Al surface could be kept clean only at $T > 1173$ K through the Al evaporation and reaction with Al_2O_3 to form volatile Al_2O. This may explain the distinct difference in the contact angles, especially the final values, at $T = 1073$ K and $T > 1073$ K, as shown in Fig. 9. On the other hand, a considerable decrease in the contact angles at 1173 K in the initial wetting stage, whose magnitude is even larger than that at 1273 K, to a great extent, may result from the disruption of the thin oxide film at the interface by the molten Al interaction or reaction with the TiAlN film and thus establishes an intimate Al–TiAlN contact.

The interaction or reaction between Al and the TiAlN film may proceed in the form of Al + TiAlN = $(Ti_{1-x}Al_x)N$ ($x > 0.5$), leading to the film at the interface being rich in Al. The outward diffusion of Ti into molten Al can further enhance this effect. As a consequence, the titanium atoms in the Ti(Al)N lattice will be substituted more by the aluminum atoms with a smaller atomic radius, making the film structure change from a cubic NaCl-structure (TiN) to a hexagonal würtzite-structure (AlN) or a mixed two-phase structure [9,24], and correspondingly, the contact angle first displays a noticeable decrease (in a short time) and then remains almost constant (Fig. 9). With respect to the values, the true contact angles (i.e., in the case of clean Al) might be in the range of 80–100° at 1173–1273 K, depending largely on the composition and/or the structure of the TiAlN (or $Ti_{1-x}Al_xN$) films. At lower temperatures, however, the measured contact angles are much larger due to the Al surface oxidation.

Another problem that needs to be concerned with is the thermal stability of the TiAlN films at 1073–1273 K. We oberved that the as-deposited bluish-black TiAlN surface exhibited no distinct color change after annealing at 1073 K but slightly turned to reddish-violet after annealing at 1173 K, and this change is more significant after annealing at 1273 K, which may correspond to

the phase decomposition of TiAlN into AlN and TiN. McIntyre et al. [25] reported the precipitation of the würtzite AlN phase from the $Ti_{0.5}Al_{0.5}N$ films after 1.5 h annealing at 1173 K. Similar results were also reported by Höring et al. [26] and Lee et al. [27] for the Al-rich $Ti_{1-x}Al_xN$ (x=0.67, 0.75 and 0.8) films but at higher annealing temperatures (T=1273–1373 K). If the phase decomposition does proceed, the wettability is expected to be improved to some extent since the precipitated phases, both AlN and TiN, are well wetted by the molten Al [28–30].

Finally, in terms of Eq. (2) and using the available values of the contact angle and surface tension of the molten Al [31], the work of adhesion for the molten Al on the TiAlN films at 1173–1273 K was estimated to be 0.77–1.08 J m^{-2}. In the case of Al being oxidized, the adhesion, however, would be significantly decreased.

5. Conclusions

We have examined the wettability, adhesion and reaction between the TiAlN films and molten Al at temperatures between 1073 K and 1273 K using an improved sessile drop method in a reducing Ar–3% H_2 atmosphere. The true wettability cannot be measured for the films deposited on the stainless steel (as well as other kinds of steels) and tungsten substrates due to the considerable interdiffusion and/or reaction between molten Al and the substrate constituents. For the films deposited on the stable alumina single crystals and in contact with clean Al, the true contact angles are in the range of 80–100° at 1173–1273 K and the work of adhesion is 0.77–1.08 J m^{-2}. In the case of oxidized Al, typically at T<1173 K, however, the wettability and the adhesion are significantly decreased.

A limited reaction between the molten Al and TiAlN may proceed at 1073–1273 K, making the TiAlN film at the interface rich in Al; on the other hand, the TiAlN as well as Al-rich $Ti_{1-x}Al_xN$ (x>0.5) films may undergo some structural changes and/or phase decomposition, yielding a certain degree of the wettability and adhesion improvement.

Acknowledgements

The authors would like to thank Mr. S. Kawaguchi, Mr. S. Masa and Dr. K. Kanda for their kind help in preparing the TiAlN films. This work was supported by the 21st Century COE Program (Project "Center of Excellence for Advanced Structural and Functional Materials Design") of the Ministry of Education, Sports, Culture, Science and Technology, Japan.

References

[1] W.D. Münz, J. Vac. Sci. Technol., A 4 (1986) 2717.
[2] O. Knotek, W.D. Münz, T. Leyendecker, J. Vac. Sci. Technol., A 5 (1987) 2173.
[3] O. Knotek, M. Böhmer, T. Leyendecker, F. Jungblut, Mater. Sci. Eng., A Struct. Mater.: Prop. Microstruct. Process. 105/106 (1988) 481.
[4] T. Leyendecker, O. Lemmer, S. Esser, J. Ebberink, Surf. Coat. Technol. 48 (1991) 175.
[5] W. Konig, R. Fritsch, D. Kammermeier, Surf. Coat. Technol. 49 (1991) 316.
[6] J.R. Roos, J.P. Celis, E. Vancoille, H. Veltrop, S. Boelens, F. Jungblut, J. Ebberink, H. Homberg, Thin Solid Films 193/194 (1990) 547.
[7] J.G. Han, J.S. Yoon, H.J. Kim, K. Song, Surf. Coat. Technol. 86/87 (1996) 82.
[8] P.C. Jindal, A.T. Santhanam, U. Schleinkofer, A.F. Schuster, Int. J. Refract. Met. Hard Mater. 17 (1999) 163.
[9] M. Zhou, Y. Makino, M. Nose, K. Nogi, Thin Solid Films 339 (1999) 203.
[10] R.M. Souto, H. Alanyali, Corros. Sci. 42 (2000) 2201.
[11] I.S. Choi, J.C. Park, Surf. Coat. Technol. 131 (2000) 383.
[12] S. Paldey, S.C. Deevi, Mater. Sci. Eng., A Struct. Mater.: Prop. Microstruct. Process. 342 (2003) 58.
[13] O. Salas, S. Carrera, K. Kearns, D. Zhong, B. Mishra, G. Mustoe, J. Moore, Ried Jr., P., North American Die Casting Association (NADCA) Congress, Rosemont, Illinois, September 30 to October 2, 2002, Paper no. T02-042.
[14] J. Moore, J. Lin, S. Carrera, O. Salas, B. Mishra, G. Mustoe, P. Ried Jr., North American Die Casting Association (NADCA) Congress, Indianapolis, Indiana, September 16–19, 2003, Paper no. T03-025.
[15] P. Shen, H. Fujii, T. Matsumoto, K. Nogi, J. Am. Ceram. Soc. 87 (2004) 2151.
[16] P. Shen, H. Fujii, T. Matsumoto, K. Nogi, Acta Mater. 51 (2003) 4897.
[17] H.P. Klug, L.E. Alexander, X-ray Diffraction Procedures: For Polycrystalline and Amorphous Materials, 2nd ed., A Wiley-Interscience Publication, John Wiley and Sons, Inc., New-York, NY, 1974.
[18] T.B. Massalski, J.L. Murray, L.H. Bennett, H. Baker, Binary Phase Diagrams, 2nd ed., ASM International, Materials Park, OH, 1990.
[19] H. Fujii, H. Nakae, K. Okada, Acta Metall. Mater. 41 (1993) 2963.
[20] H. John, H. Hausner, J. Mater. Sci. Lett. 5 (1986) 549.
[21] V. Laurent, D. Chatain, C. Chatillon, N. Eustathopoulos, Acta Metall. 36 (1988) 1797.
[22] S.W. Ip, M. Kucharski, J.M. Toguri, J. Mater. Sci. Lett. 12 (1993) 1699.
[23] D.J. Wang, S.T. Wu, Acta Metall. Mater. 42 (1994) 4029.
[24] U. Wahlström, L. Hultman, J.E. Sundgren, F. Adibi, I. Petrov, J.E. Greene, Thin Solid Films 235 (1993) 62.
[25] D. McIntyre, J.E. Greene, G. Håkansson, J.E. Sundgren, W.D. Münz, J. Appl. Phys. 67 (1990) 1542.
[26] A. Höring, L. Hultman, M. Odén, J. Sjölén, L. Karlsson, J. Vac. Sci. Technol., A 20 (2002) 1815.
[27] S.H. Lee, B.J. Kim, H.H. Kim, J.J. Lee, J. Appl. Phys. 80 (1996) 1469.
[28] S.K. Rhee, J. Am. Ceram. Soc. 53 (1970) 386.
[29] H.N. Ho, S.T. Wu, Mater. Sci. Eng., A Struct. Mater.: Prop. Microstruct. Process. 248 (1998) 120.
[30] G.R. Prin, T. Baffie, M. Jeymond, N. Eustathopoulos, Mater. Sci. Eng., A Struct. Mater.: Prop. Microstruct. Process. 298 (2001) 34.
[31] P. Shen, H. Fujii, T. Matsumoto, K. Nogi, J. Mater. Sci. 40 (2005) 2329.